Article

Cell Reports

Acetylation of an NB-LRR Plant Immune-Effector Complex Suppresses Immunity

Graphical Abstract

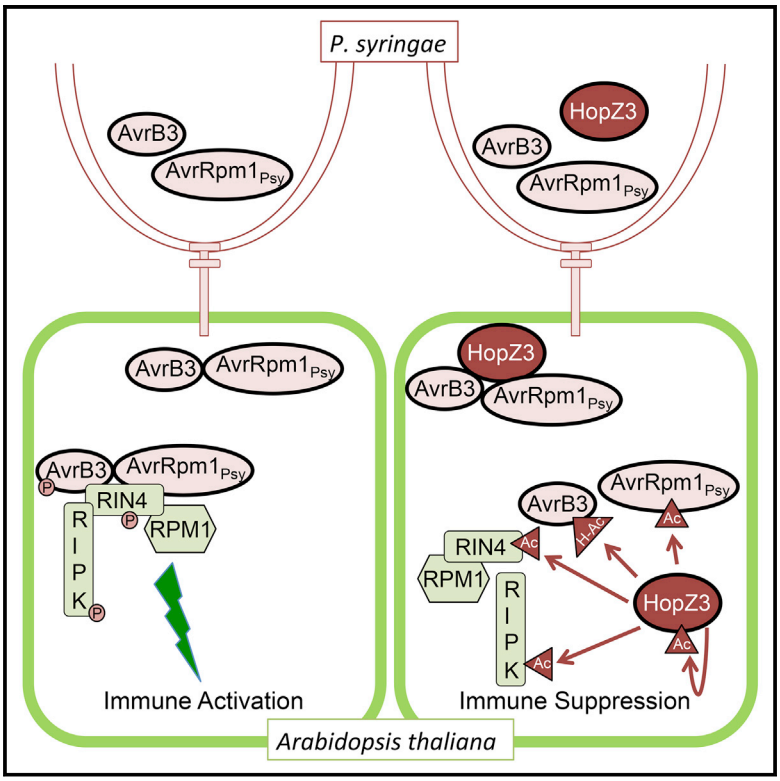

Highlights

- HopZ3 targets the RPM1 immune complex and effectors that activate this complex
- HopZ3 acetylates Ser, Thr, Lys, as well as His
- HopZ3 acetylates residues important for multiple facets of plant immune signaling
- Bacterial effector-effector interactions are implicated in the outcome of infection

Authors

Jiyoung Lee, Andrew J. Manning, Donald Wolfgeher, ..., Richard W. Michelmore, Stephen J. Kron, Jean T. Greenberg

Correspondence

jgreenbe@uchicago.edu

In Brief

Lee et al. find that the *P. syringae* type III effector HopZ3 suppresses plant defense by acetylating multiple members of the RPM1 immune complex and its triggering effectors. HopZ3 uses a novel multi-faceted approach by altering kinase activity, blocking phosphorylation, and disrupting protein-protein interactions, thus robustly suppressing immunity.

Lee et al., 2015, Cell Reports *13*, 1670–1682
November 24, 2015 ©2015 The Authors
http://dx.doi.org/10.1016/j.celrep.2015.10.029

OPEN ACCESS
CellPress

Cell Reports
Article

Acetylation of an NB-LRR Plant Immune-Effector Complex Suppresses Immunity

Jiyoung Lee,[1,3] Andrew J. Manning,[1] Donald Wolfgeher,[1] Joanna Jelenska,[1] Keri A. Cavanaugh,[2] Huaqin Xu,[2] Sandra M. Fernandez,[1] Richard W. Michelmore,[2] Stephen J. Kron,[1] and Jean T. Greenberg[1,*]

[1]Department of Molecular Genetics and Cell Biology, University of Chicago, Chicago, IL 60637, USA
[2]The Genome Center & Department of Plant Sciences, University of California, Davis, Davis, CA 95616, USA
[3]Present address: Plant Systems Engineering Research Center, Korea Research Institute of Bioscience and Biotechnology, 125 Gwahak-ro, Yuseong-gu, Daejeon 305-806, Korea
*Correspondence: jgreenbe@uchicago.edu
http://dx.doi.org/10.1016/j.celrep.2015.10.029

SUMMARY

Modifications of plant immune complexes by secreted pathogen effectors can trigger strong immune responses mediated by the action of nucleotide binding-leucine-rich repeat immune receptors. Although some strains of the pathogen *Pseudomonas syringae* harbor effectors that individually can trigger immunity, the plant's response may be suppressed by other virulence factors. This work reveals a robust strategy for immune suppression mediated by HopZ3, an effector in the YopJ family of acetyltransferases. The suppressing HopZ3 effector binds to and can acetylate multiple members of the RPM1 immune complex, as well as two *P. syringae* effectors that together activate the RPM1 complex. These acetylations modify serine, threonine, lysine, and/or histidine residues in the targets. Through HopZ3-mediated acetylation, it is possible that the whole effector-immune complex is inactivated, leading to increased growth of the pathogen.

INTRODUCTION

Post-translational modifications (PTMs) can modulate protein activity, stability, interactions with other macromolecules, and subcellular localization (Karve and Cheema, 2011; Salomon and Orth, 2013). PTMs are often rapidly acquired, reversible, and highly regulated (Deribe et al., 2010). In plant defense responses to pathogenic bacteria, phosphorylation, a common PTM, can play a critical role in the early stages of signal transduction. For example, in response to a fragment of bacterial flagellin called flg22, the flagellin receptor (FLS2) becomes rapidly phosphorylated, which is important for downstream signaling events that confer disease resistance (Asai et al., 2002). Phosphorylation also can be important for immunity conferred through complexes that contain intracellular nucleotide binding-leucine-rich repeat (NB-LRR) receptor proteins encoded by resistance genes (Ellis and Dodds, 2003; Liu et al., 2011; Oh and Martin, 2011). Some NB-LRR protein complexes contain kinases that are important for sensing type III secreted effectors and can lead to receptor-mediated immune signaling (e.g., RPM1/RIPK and PRF/PTO) (Liu et al., 2011; Mucyn et al., 2006).

NB-LRR proteins are triggered to signal upon direct binding or indirect interactions with a limited number of specific cognate pathogen effectors (Chisholm et al., 2006; Deslandes and Rivas, 2012; Jones and Dangl, 2006). Several type III-secreted effectors from the bacterial pathogen *P. syringae* activate NB-LRRs by modifying proteins that bind to NB-LRRs (Bent et al., 1994; Grant et al., 1995; Simonich and Innes, 1995). One such NB-LRR-interacting protein is RIN4, an intrinsically disordered hub protein that interacts with several components of the RPM1 defense complex (Sun et al., 2014). RIN4 is a major target of effector modification (Liu et al., 2011; Mackey et al., 2002, 2003; Wilton et al., 2010). In *Arabidopsis*, when effectors either stimulate RIN4 phosphorylation of threonine 166 (RIN4-pT166) or cleave RIN4, signaling is activated through the NB-LRRs RPM1 or RPS2, respectively (Liu et al., 2011; Mackey et al., 2002, 2003).

Some bacterial effectors from plant pathogens can be identified by their ability to trigger plant immunity when expressed in heterologous pathogen strains. This approach works because the immune-inducing activity is usually phenotypically dominant to the virulence activities of other effectors (Gabriel et al., 1986; Shen and Keen, 1993; Staskawicz et al., 1984; Whalen et al., 1988). However, the activity of an immune-inducing effector can be masked by the presence of other effectors encoded by the same bacteria (Tsiamis et al., 2000; Szczesny et al., 2010). By studying effectors from the same or different strains on the same plant, it has been shown that some effectors can suppress cell death induced by multiple effectors (Jamir et al., 2004; Vinatzer et al., 2006). Additionally, cell death induced by a single effector can be suppressed by multiple effectors from the same strain (Guo et al., 2009). Understanding the basis of this within-strain masking is important for discerning the mechanism of pathogenesis and predicting changes in pathogenicity in the field due to the acquisition or loss of effectors.

P. syringae pv. *syringae* strain B728a (*Psy*B728a) grows both epiphytically (associated with plant epidermal cells) and endophytically (associated with plant mesophyll cells), in a manner that depends on type III effectors (Hirano et al., 1999; Lee et al., 2012b; Vinatzer et al., 2006). Transient expression of pairs

of effectors from *Psy*B728a in *Nicotiana benthamiana* showed that the HopZ3 effector can suppress cell death induced by at least four other *Psy*B728a effectors (Vinatzer et al., 2006). Furthermore, *Psy*B728a lacking HopZ3 (*Psy*Δ*hopZ3*) shows reduced growth on *Arabidopsis* and tomato (Lee et al., 2012b; Vinatzer et al., 2006), suggesting that HopZ3 normally suppresses effector-induced immunity in these plants.

HopZ3 is a member of the YopJ family of effectors, which are found in many plant and animal pathogens (Lewis et al., 2011). YopJ family members typically require conserved histidine (His) and cysteine (Cys) residues proposed to be important for catalysis (Lee et al., 2012b; Lewis et al., 2011; Mukherjee et al., 2006). YopJ and VopA, effectors of *Yersinia pestis* and *Vibrio parahaemolyticus,* respectively, acetylate mitogen-activated kinase kinases to block host immunity (Mittal et al., 2010; Mukherjee et al., 2006; Trosky et al., 2007). Both YopJ and VopA can acetylate lysine (Lys), serine (Ser), and threonine (Thr) in target proteins (Mukherjee et al., 2006; Trosky et al., 2007). A common feature of several YopJ family proteins is that their acetyltransferase activities are strongly stimulated by the eukaryotic co-factor inositol hexakiphosphate (IP_6) (Lee et al., 2012a; Ma et al., 2015; Mittal et al., 2010).

Only one YopJ family effector from a bacterial plant pathogen (PopP2 from *Ralstonia solanacearum*) was shown to cause in planta acetylation of a substrate (Le Roux et al., 2015; Sarris et al., 2015). Two other YopJ family proteins from plant pathogens, HopZ1a from *P. syringae* and AvrBsT from *Xanthomonas euvesicatoria*, also were found to have acetyltransferase activity in vitro on one or more potential substrates. Acetylation activity requires the conserved catalytic Cys or His (Cheong et al., 2014; Jiang et al., 2013; Lee et al., 2012a; Lewis et al., 2013).

This study addresses the mechanism of HopZ3 immune suppression in *Arabidopsis* through acetylation of multiple targets. We propose that modification of several components in a plant-effector complex can explain how immunity is attenuated.

RESULTS

HopZ3 Interacts with Multiple Members of an Immune Complex as well as Additional Defense Proteins

To find clues about how HopZ3 promotes *Psy*B728a growth in *Arabidopsis* (Vinatzer et al., 2006), we mined data from ongoing high-throughput experiments in which interactions between and among libraries of pathogen effectors and plant immune-signaling components were tested pairwise in targeted Y2H mating assays. We also performed a genome-wide Y2H screen with HopZ3 as the bait (Figure S1A; Table S1).

HopZ3 interacted with the *Arabidopsis* proteins RIN4 and several kinases, most of which belong to the receptor-like cytoplasmic kinase (RLCK) family (members RIPK, PBS1, BIK1, and PBL1) and one of which is a mitogen-activated protein kinase, MPK4 (Figure S1A; Table S1). Interestingly, HopZ3 also interacted with the *Psy*B728a effectors AvrB3 and AvrRpm1$_{Psy}$ as well as proteins encoded by orthologous alleles of these proteins from other *P. syringae* strains (AvrB and AvrRpm1, respectively). However, HopZ3 did not interact with itself or the HopI1$_{Psy}$ effector (Figure S1A; Table S1). For selected proteins, we confirmed that they were expressed in yeast, including HopI1$_{Psy}$, the negative control in the Y2H assay (Figure S1B).

Using bimolecular fluorescence complementation (BIFC), co-immunoprecipitation (coIP), and/or pull-down assays, we corroborated many of the positive Y2H protein-protein interactions either in planta or in vitro (Figures 1A and 1B; Figures S1C–S1E; Table S1). HopZ3 did not interact with itself or HopI1$_{Psy}$ as assayed by either BIFC or pull-down (Figures 1A and 1B). Some HopZ3 interactors previously were shown to form complexes (e.g., RIN4-RIPK, RIPK-AvrB, RIN4-AvrB, RIN4-AvrRpm1, AvrB-MPK4, and RIN4-MPK4) (Cui et al., 2010; Liu et al., 2011; Mackey et al., 2002). Interestingly, *Psy*B728a effectors that bound to HopZ3 also could bind to each other (e.g., AvrB3-AvrRpm1$_{Psy}$, AvrB3-AvrB3, and AvrRpm1$_{Psy}$-AvrRpm1$_{Psy}$) (Figure S1A; Table S1).

As several components of RPM1 immune complexes (e.g., RIN4, RIPK, AvrB, and AvrRpm1) were among the HopZ3 interactors, we tested whether the virulence effect of HopZ3 depended on RPM1. In *rpm1* plants, *Psy*Δ*hopZ3* and a complemented strain expressing HopZ3 grew to the same level as bacteria-expressing HopZ3 in wild-type (WT) plants. Thus, HopZ3 promotes bacterial growth by suppressing RPM1 immunity (Figure 1C).

Interacting Partners Direct HopZ3 to the Cell Periphery

Using the BIFC results as an indicator of localization, most of the interactions between HopZ3 and other proteins, except for the HopZ3-MPK4 interaction, occurred at the cell periphery (Figure 1A; Figure S1F). This fits with the fact that most HopZ3-interacting proteins function at the plasma membrane (Kim et al., 2005; Liu et al., 2011; Nimchuk et al., 2000). HopZ3 expressed on its own in plants is mainly cytoplasmic and nuclear (Lee et al., 2012b; Lewis et al., 2008). The lack of membrane localization could be due to the competition between higher endogenous levels of cytosolic/nuclear (e.g., MPK4) (Andreasson et al., 2005) versus membrane protein interactors (e.g., RIPK/RIN4) (Kim et al., 2005; Liu et al., 2011).

To further test whether an interactor can change the subcellular location of HopZ3, we used a fractionation approach with fusion versions of HopZ3 and AvrB3 that retain their biological activity in planta (Lee et al., 2012b; Vinatzer et al., 2006). AvrB3, like AvrB, contains a predicted N-terminal myristoylation motif that targets the protein to the plant plasma membrane (Nimchuk et al., 2000). To investigate whether the presence of AvrB3 alters the localization of HopZ3, we mutated the myristoylation site in AvrB3 to create a Gly to Ala (G2A) substitution. The G2A mutation caused mislocalization of the AvrB3-GFP fusion protein (Figure S2A). Simultaneous co-expression of HopZ3 with AvrB3 directly in plants caused HopZ3 to partition with the membrane fraction (Figure 1D). However, when AvrB3_G2A was co-expressed with HopZ3, membrane localization was mostly lost (Figure 1D). Thus, at least one interacting effector from *Psy*B728a can stably recruit HopZ3 to the membrane fraction. Together with the HopZ3-AvrB3 BIFC signal at the cell periphery, the fractionation analysis of HopZ3 in the presence of AvrB3 is consistent with the known location of RPM1 components.

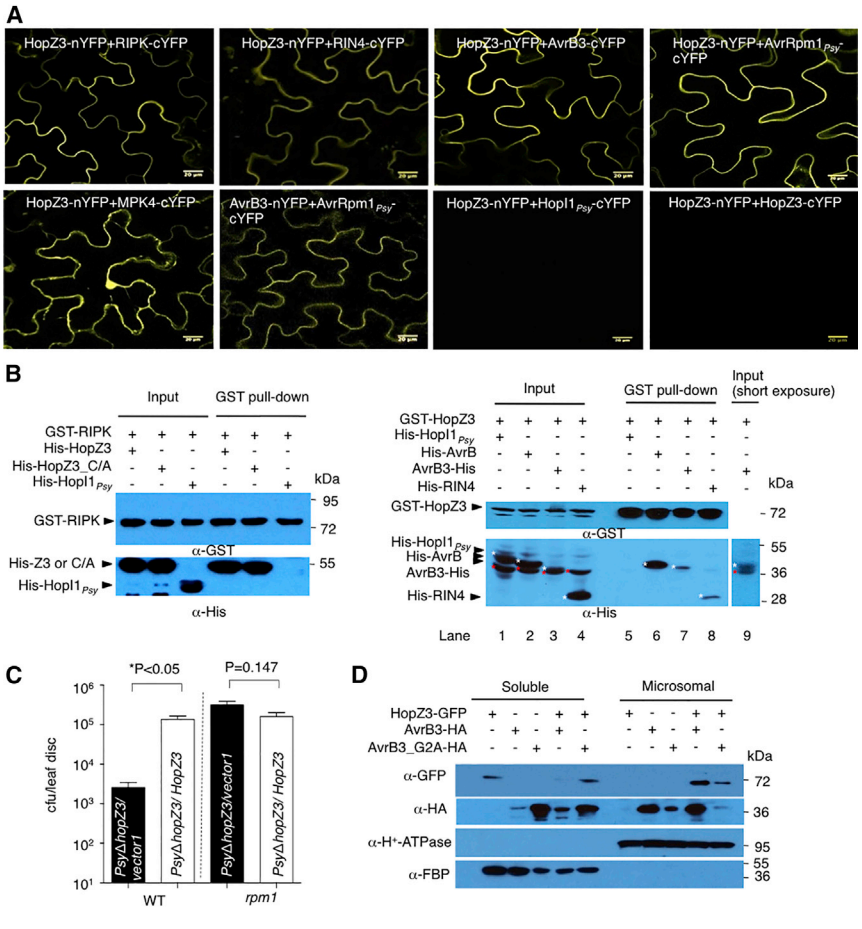

Figure 1. HopZ3 Interacts with RIN4, RIPK, AvrRpm1$_{Psy}$, and AvrB/B3

(A) Reconstituted YFP fluorescence (BIFC) of constructs coexpressed in *N. benthamiana* was monitored 2 days after transformation. HopZ3-nYFP with Hopl1$_{Psy}$-cYFP or HopZ3-cYFP was used as a negative control. Bar represents 20 μm. See also Figure S1E and Table S1.

(B) HopZ3 directly interacts with RIPK, AvrB, AvrB3, and RIN4. (Left) In vitro pull-down assays with purified recombinant GST-RIPK and His-HopZ3 (Z3), His-HopZ3_C300A (C/A), or His-Hopl1$_{Psy}$ (I1) are shown. The presence of HopZ3 variants in the GST pull-down was detected with His antibody. (Right) Recombinant GST-HopZ3 immobilized on gluthathione agarose was incubated with extracts from *E. coli* expressing His-tagged AvrB, AvrB3, RIN4, or control Hopl1$_{Psy}$. Proteins pulled down were detected with GST (top) and His (bottom) antibodies. Expected proteins are marked by white asterisks and the background band by a red asterisk. Note that the expected size of AvrB3-His is similar to the background band (lane 3). In shorter exposure (lane 9), AvrB3 can be distinguished from the background band.

(C) HopZ3 inhibits RPM1-mediated defense. Col (WT) and *rpm1* leaves were infiltrated with *Psy*Δ*hopZ3* containing empty vector pME6010 (vector 1) or HopZ3. *Psy*Δ*hopZ3*/vector1 had growth defect only in Col (WT) 3 days post-infiltration (dpi). Error bars are SE (n = 8; *p < 0.5, t test).

(D) AvrB3 and HopZ3 co-localize in microsomal fraction. HopZ3-GFP was detected mostly in the soluble fraction when transiently expressed in *N. benthamiana* alone or with AvrB3_G2A-HA (myristoylation mutant), but it was present mostly in the microsomal fraction when expressed with AvrB3-HA. Expressed proteins were detected with GFP and HA antibodies. H^+-ATPase and fructose-1,6-bisphosphatase (FBP) served as markers for membrane and soluble proteins, respectively. See also Figure S1 and Table S1.

RPM1-Mediated Immunity Is Activated by AvrB3 and AvrRpm1$_{Psy}$

Two HopZ3 interactors (AvrB3 and AvrRpm1$_{Psy}$) are homologs of effectors (AvrB and AvrRpm1, respectively) that stimulate RPM1 immunity (Bisgrove et al., 1994; Liu et al., 2011; Mackey et al., 2002; Ritter and Dangl, 1995). One possibility to explain why *Psy*Δ*hopZ3* has reduced growth relative to *Psy*B728a is that AvrB3 and/or AvrRpm1$_{Psy}$ trigger RPM1 immunity that is normally inhibited by HopZ3.

We first assessed if AvrB3 and AvrRpm1$_{Psy}$ trigger RPM1-dependent signaling using a heterologous *P. syringae* strain that lacks these effectors. We monitored the growth of *P. syringae* pv. *tomato* DC3000 (*Pto*DC3000) expressing AvrB3 (*Pto*DC3000/AvrB3) in WT or *rpm1*-deficient plants. AvrB3 suppressed growth of *Pto*DC3000 only in the WT background, indicating that it triggers RPM1-dependent signaling (Figure 2A). However, the AvrB3_G2A mutant that was mislocalized due to the lack of its myristoylation site (Figure 1D) did not inhibit bacterial growth (Figure 2A). As expected, *Pto*DC3000/AvrB3 induced RIN4-pT166 after infection, a hallmark of RPM1-mediated signaling. However, the level of RIN4-pT166 was not as high as that found after *Pto*DC3000/AvrB infection (Figure 2B). In Y2H and in planta BIFC assays, AvrB3 interacted with both RIPK and RIN4 (Figures S1A and S2B). Thus, AvrB3 has many similar effects as reported for AvrB (Liu et al., 2011; Mackey et al., 2002). Unlike AvrB3, *Pto*DC3000 expressing AvrRpm1$_{Psy}$ (*Pto*DC3000/AvrRpm1$_{Psy}$) did not induce detectable growth suppression or RIN4-p166 after infection (Figures 2B and 2C).

We next assessed the roles of AvrB3 and AvrRpm1 using various deletion mutants of *Psy*B728a. Deletion of AvrB3, AvrRpm1$_{Psy}$, or both effectors did not change the in planta growth of bacteria (Figure 2D). However, compared with *PsyΔhopZ3*, a strain that also lacked AvrB3, AvrRpm1$_{Psy}$ or both effectors showed increased growth (Figure 2D). This suggests that AvrB3 and AvrRpm1$_{Psy}$ must be delivered together from their native strain to activate immunity, possibly due to their interaction (Figure 1A; Figure S1A). The increased growth of *PsyΔhopZ3ΔavrRpm1*$_{Psy}$ or *PsyΔhopZ3ΔavrB3* was complemented by plasmid-borne copies of AvrRpm1$_{Psy}$ or AvrB3, respectively (Figure 2E).

Finally, we tested the effect of expressing HopZ3 directly in *Arabidopsis* (Figure S2C). These plants promoted the growth of strains that are usually suppressed by RPM1 signaling (*Pto*DC3000/AvrB and *Pto*DC3000/AvrRpm1). The effect of

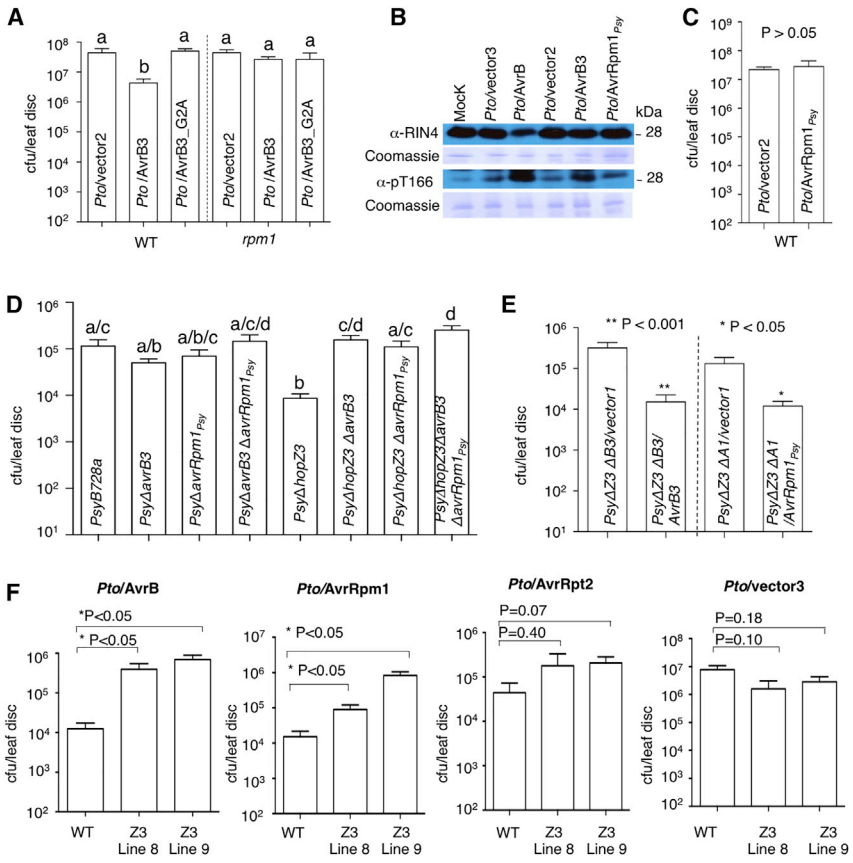

Figure 2. HopZ3 Suppresses Recognition of Effectors that Trigger RPM1 Signaling

(A) Immunity induced by AvrB3 requires RPM1 in *Arabidopsis*. Col (WT) and *rpm1* leaves were infiltrated with *Pto*DC3000 expressing AvrB3, AvrB3_G2A, or an empty vector. Only *Pto*/AvrB3 strain had a growth defect in WT plants 3 dpi. Different letters indicate significant difference ($p < 0.05$, ANOVA and Fisher's least significant difference [LSD] test; n = 12).

(B) The RIN4 T166 phosphorylation by *Pto*DC3000 expressing AvrB3 and AvrRpm1$_{Psy}$. Col (WT) plants were infiltrated with OD_{600} = 0.1 of *Pto*DC3000 containing an empty vector, AvrB (positive control), AvrB3, and AvrRpm1$_{Psy}$. Proteins were extracted 5 hr after infection and immunoblots were performed with RIN4 or phospho-RIN4 T166 (pRIN4) antibodies.

(C) *Arabidopsis* does not recognize *Pto* DC3000 expressing AvrRpm1$_{Psy}$. Growth of *Pto*/AvrRpm1$_{Psy}$ was not significantly different from *Pto*/vector 3 dpi (n = 12; $p > 0.05$, t test).

(D) Bacterial growth inhibition of *Psy*Δ*hopZ3* bacteria depends on AvrB3 and AvrRpm1$_{Psy}$. Growth of *Psy*Δ*avrB3*, *Psy*Δ*avrRpm1*$_{Psy}$, and *Psy*Δ*avrB3*Δ*avrRpm1*$_{Psy}$ strains was not significantly different from the WT *Psy*B728a in WT (Col) plants. *Psy*Δ*hopZ3*Δ*avrB3*, *Psy*Δ*hopZ3*Δ*avrRpm1*$_{Psy}$, and *Psy*Δ*hopZ3*Δ*avrB3*Δ*avrRpm1*$_{Psy}$ mutants grew better than *Psy*Δ*hopZ3* in WT plants 3 dpi (ANOVA, Fisher's LSD, different letters indicate significant difference $p < 0.05$; n = 20–28).

(E) Mutant complementation analysis of the effectors AvrB3 and AvrRpm1$_{Psy}$. *Psy*B728a-derivative strains were infiltrated into Col (WT) plant leaves. The growth of *Psy*Δ*Z3*Δ*B3* and *Psy*Δ*Z3*Δ*A1*$_{Psy}$ strains expressing AvrB3 or AvrRpm1$_{Psy}$ was significantly reduced compared to vector controls 3 dpi (**$p < 0.001$, *$p < 0.05$, t test; n = 16).

(F) HopZ3 interferes with recognition of AvrRpm1 and AvrB. WT and HopZ3-expressing *Arabidopsis* (Z3 line 8 and Z3 line 9) were infiltrated with *Pto*DC3000 expressing AvrB, AvrRpm1, AvrRpt2, or empty vector. These experiments were performed at the same time. Note the increased growth of *Pto*/AvrB and *Pto*/AvrRpm1 in plants that produce HopZ3 (*$p < 0.05$, t test; n = 8).

In all graphs, the following apply: *Pto*, *Pto*DC3000; *Psy*, *Psy*B728a; vector2, pME6012; vector 3, pVSP61; and error bars, SE. See also Figure S2.

HopZ3 was specific, as it did not affect the growth of *Pto*DC3000/AvrRpt2, which triggers the RPS2 immune receptor, or *Pto*DC3000/vector with no known effectors that trigger immunity in *Arabidopsis* (Figures 2F–2I). Thus, HopZ3 suppresses immunity triggered by effectors that activate RPM1 signaling.

HopZ3 Acetylates a Subset of Interacting Proteins and Its Activity Is Needed for Promoting *P. syringae* Growth on *Arabidopsis*

As HopZ3 is a member of the YopJ effector family, we tested whether it can acetylate interacting proteins. Using in vitro assays with ^{14}C acetyl-CoA, we first established that HopZ3 has autoacetylation activity that is strongly stimulated by the cofactor IP_6 and dependent on the predicted catalytic Cys residue (C300) (Figure 3A). This is consistent with a recent report that only tested HopZ3 autoacetylation activity in the presence of IP_6 in vitro (Ma et al., 2015). As expected, C300 was essential for HopZ3 to promote both endophytic and epiphytic growth of *Psy*B728a on *Arabidopsis* (Figures 3B and 3C). HopZ3 also transacetylated the interacting plant proteins RIN4, RIPK, PBS1, and BIK1 and the effectors AvrB and AvrB3 (Figures 3D and 3E; Figures S3A and S3B). As AvrRpm1$_{Psy}$ was insoluble when expressed in *E. coli*, we used liquid chromatography-tandem mass spectrometry (LC-MS/MS) analysis of proteins produced in planta to show that it was a HopZ3 substrate (Table 1).

The HopZ3 interactor MPK4 (Figure S3C), as well as the non-interactor control HopI$_{Psy}$ (Figure 3E; Figure S3C), was not acetylated by HopZ3. This indicates specificity of the acetyltransferase activity of HopZ3, despite the diversity in substrates. Additionally, immunoprecipitation of transiently expressed HopZ3, but not HopZ3_C300A, followed by immunoblotting with an acetyl-lysine antibody showed that only WT HopZ3 was acetylated in planta (Figure 1F).

Thus, HopZ3 has acetyltransferase activity both in vitro and within plant cells. Furthermore, the activity is needed for the virulence effect of HopZ3.

Identification of Acetylation Sites in the HopZ3 Substrates

To gain insight into how HopZ3 might block immunity and to confirm that acetylation of substrates occurs in planta, we determined the modification sites from HopZ3-acetylated proteins

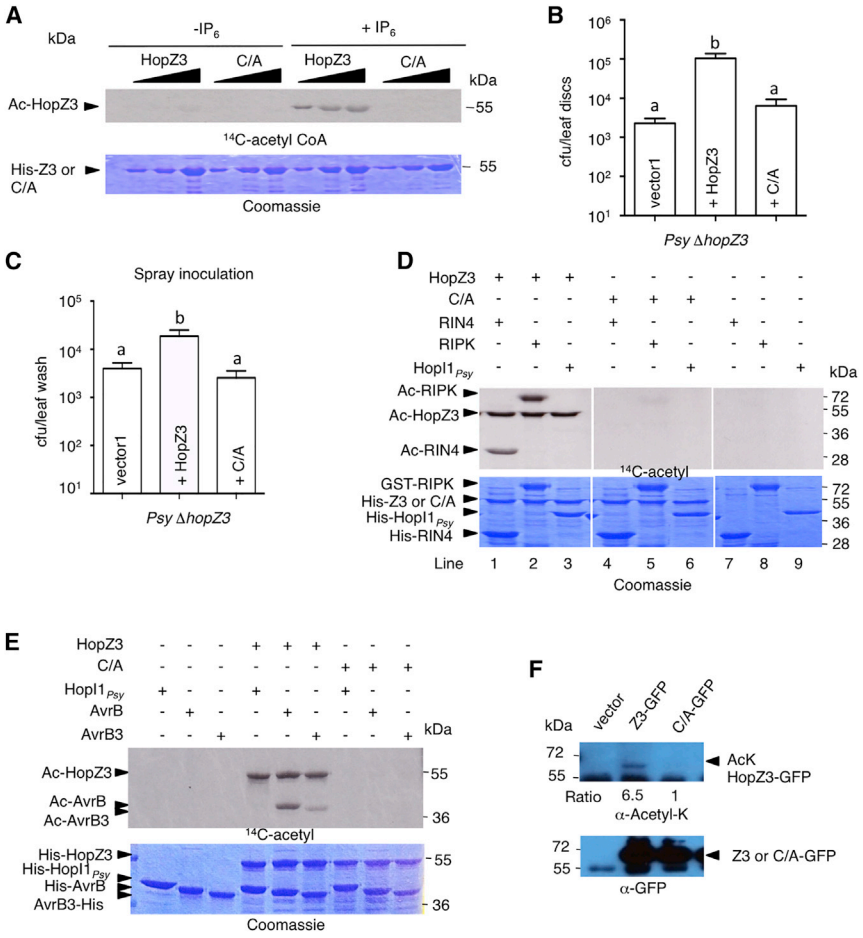

Figure 3. HopZ3 Acetylates Itself and Many HopZ3-Interacting Proteins

(A) In vitro autoacetylation of His-HopZ3 (Z3) and His-HopZ3_C300A (C/A) proteins in the presence or absence of IP_6 (inositol hexakisphosphate). Progressively higher amounts (0.5–2 μg) of purified His-HopZ3 or His-HopZ3 _C300A (C/A) were incubated with [^{14}C]-acetyl-CoA for 2 hr at RT, separated by SDS-PAGE, and autoradiographed.

(B) The C300 residue in HopZ3 is required for virulence. Only the bacterial population of *PsyΔhopZ3*/HopZ3 in Col was increased compared to *PsyΔhopZ3*/vector1 3 dpi (ANOVA, Fisher's LSD, different letters indicate significant difference $p < 0.5$; $n = 8$).

(C) HopZ3 promotes epiphytic bacterial growth on Col. *PsyΔhopZ3* expressing HopZ3 or HopZ3_C300A was sprayed onto *Arabidopsis*. Only bacterial population of *PsyΔhopZ3* was higher than vector control (ANOVA, Fisher's LSD; $n = 24$).

(D and E) HopZ3 acetylates RIPK, RIN4, AvrB, and AvrB3. Purified recombinant His-tagged substrates were incubated with His-HopZ3 or His-HopZ3_C300A in the presence of [^{14}C]-labeled acetyl-CoA and IP_6. Acetylated proteins were detected by autoradiography. In (D), lanes 1–6 are from one exposure of one continuous gel. Samples in lanes 7–9 were run together and exposed at the same time as lanes 1–6.

(F) HopZ3 is acetylated in planta. HopZ3-GFP variants transiently expressed in *N. benthamiana* were immunoprecipitated with GFP antibodies and detected by immunoblotting (top, anti-acetylated Lys; and bottom, anti-GFP). Protein levels were estimated by densitometry using ImageJ (Gassmann et al., 2009) and expressed as a ratio. See also Figure S3.

using LC-MS/MS. To map acetylation sites on substrates, we used both an in planta approach as well as in vitro assays with recombinant proteins. For the in planta approach, we transiently co-expressed HopZ3 and each substrate in *N. benthamiana* followed by immunoprecipitation of the substrate. For in vitro assays, we developed a heavy isotope approach using ^{13}C acetyl-CoA to isotope label acetylation sites. This allowed us to distinguish HopZ3-dependent acetylation from background acetylation that may have occurred during protein production in *E. coli*. For both approaches, HopZ3_C300A was used as a control.

Mapped acetylation sites in RIPK, AvrB3, AvrRpm1$_{Psy}$, and RIN4 are shown in Table 1. In all cases, multiple acetylation sites were found in the substrates. The majority of acetylation sites in most substrates corresponded to conserved residues in paralogous or homologous proteins (Table 1). In addition to Ser, Thr, and Lys modifications in several substrates, we found a His acetylation site in AvrB3 (H221) (Table 1; Figure S4).

Some acetylation sites found in planta were absent in vitro. Therefore, we examined our data for phosphorylation sites that might competitively block acetylation (Table 1; Tables S2 and S3). S251, T252, and T257 of RIPK were phosphorylated in protein produced in *E. coli* and used for in vitro reactions (Table 1). By contrast, these sites were acetylated by HopZ3 in planta (Table 1). Thus, phosphorylation of S251, T252, and T257 in RIPK in vitro blocks their modification by HopZ3 (Table 1; Table S3).

Structural modeling of RIPK and AvrB3 suggests that HopZ3-mediated acetylation is targeted to important sites of either catalysis or protein-protein interaction. Several of the acetylation sites in RIPK were in structural proximity to the ATP-binding site (K122, T164, S174, and S221), as well as within the nearby activation loop (S251 and T252) (Figures 4A and 4B). Strikingly, two of the acetylation sites in AvrB3 (H221 and T137) (Figures 4C and 4D) correspond to residues in AvrB (H217 and T125) that form a small hydrogen-bonding network with T166 in RIN4 (Desveaux et al., 2007). The interaction of AvrB with RIN4 and RIPK is known to be reduced when T125 is mutated (Desveaux et al., 2007; Liu et al., 2011). These observations suggest that HopZ3-mediated acetylation may functionally affect the targets through multiple mechanisms.

Acetylation Sites in AvrB3 Are in Residues Important for Immune Elicitation

Based on acetylation mapping, we hypothesized that HopZ3 modifies sites in other effectors that could be important for recognition and/or activation of immunity. We tested this idea

Table 1. MS/MS Acetylated Residues that Depend on the Catalytic Activity of HopZ3; See Also Figure S4, Supplemental Experimental Procedures, Data S1 and Tables S2 and S3

HopZ3-Interacting Proteins[a]	Acetylation Site[b]	Z3/Z3_C/A Enrichment In Vitro[c]	Z3/Z3_C/A Enrichment In Planta[c]	Phospho[d]	Conserved Sites in Paralogous or Homologous Proteins[e]
RIPK i.v. (64%) i.p. (62%)	S11	>10	1.1	i.v.	2/3
	S47	NM	>10	NM	0/3
	K122	>10	NR	NM	3/3
	T137	1.0	>10	NM	2/3
	T164	1.4	>10	NM	0/3
	S174	1.9	6.5	NM	3/3
	S184	NM	3.8	NM	0/3
	S221	1.1	8.7	NM	3/3
	S251	1.1	>10	i.v.	3/3
	T252	1.1	>10	i.v.	3/3
	T257	NM	>10	NM	3/3
RIN4 i.v. (86%) i.p. (78%)	K8	2.7	NR	NM	6/7
	S47	2.0	>10	i.p./i.v.	2/7
	S49/51	1.5	1.4	NM	2/7, 0/7
	S79	1.0	>10	NM	5/7
	S83	1.1	>10	NM	0/7
	K86	>10	>10	NM	4/7
	S160	1.3	5.7	NM	3/7
	S177/S178	2.9	1.2	NM	0/7, 2/7
AvrB3 i.v. (67%) i.p. (80%)	S19	1.0	2.0	NM	2/4
	T137	1.2	>10	NM	4/4
	T185	NM	>10	NM	3/4
	H221	>10	2.2	NM	4/4
	K229	NM	2.5	NM	2/4
	T306	>10	2.5	NM	2/4
AvrRpm1$_{Psy}$ i.p. (79%)	T137	ND	12.8	NM	4/4
	T152	ND	3.5	NM	1/4[f]

[a]Coverage of substrates indicated for either in vitro (i.v.) or in planta (i.p.).
[b]Sites were determined either in vitro using purified recombinant HopZ3/HopZ3_C300A and each substrate in the presence of IP_6 and C^{13}-Acetyl-CoA or in planta by co-expressing HopZ3/HopZ3_C300A and each substrate in *N. benthamiana*, followed by immunoprecipitation of the substrate.
[c]Enrichment of acetylation sites was determined by comparing the summed maximum intensity of the isotopic distribution of the same acetylated peptide in all three samples (containing HopZ3, HopZ3_C300A, or substrate alone). If the peptide modified by HopZ3 was not modified in either HopZ3_C300A or substrate-alone samples, the sites were labeled as enriched >10. The values displayed are from comparing intensity of signals from samples that contain HopZ3 versus HopZ3_C300A. NM, peptide recovered but not modified; NR, peptide not recovered; ND, not determined.
[d]Phosphorylation status of residue is as follows: i.v., in vitro; i.p., in planta; and NM, not modified.
[e]Sequence conservation at each site with paralogous or homologous proteins using Clustal W. Number of paralogous or homologous proteins analyzed in which the site was conserved is given (see the Supplemental Experimental Procedures and Data S1).
[f]In other AvrRpm1 alleles, the cognate amino acid was S (see the Supplemental Experimental Procedures and Data S1).

for AvrB3, since we could model its structure based on a known crystal structure of AvrB with a fragment of RIN4. Previous mutational analysis of H217 and T125 in AvrB (RIN4-contacting residues) (Desveaux et al., 2007) indicated that these residues are important for inducing cell death (both) and/or reduced bacterial growth (T125) (Desveaux et al., 2007). Site-directed mutation of H221 or T137 abolished the ability of AvrB3 to suppress bacterial growth during infection, but did not affect the stability of the proteins in *Psy*B728a (Figure 5A). Thus, at least some HopZ3-mediated acetylation sites affect key functional residues in AvrB3.

Acetylation of Plant Immune Components by HopZ3 Affects Their Activity

RIPK and RIN4 are key players in the activation of RPM1 immunity (Liu et al., 2011; Walter et al., 2004). Thus, we tested how acetylation might affect their activity and function, respectively. Using radiolabeled ATP, RIPK autophosphorylation was unaffected by HopZ3_C300A, but was greatly inhibited after acetylation by HopZ3 (Figure 6A). Importantly, acetylation of RIPK greatly reduced its ability to phosphorylate RIN4, a known substrate (Figure 6B). Additionally, we noticed that HopZ3_C300A was a substrate of RIPK, as evidenced by incorporation of

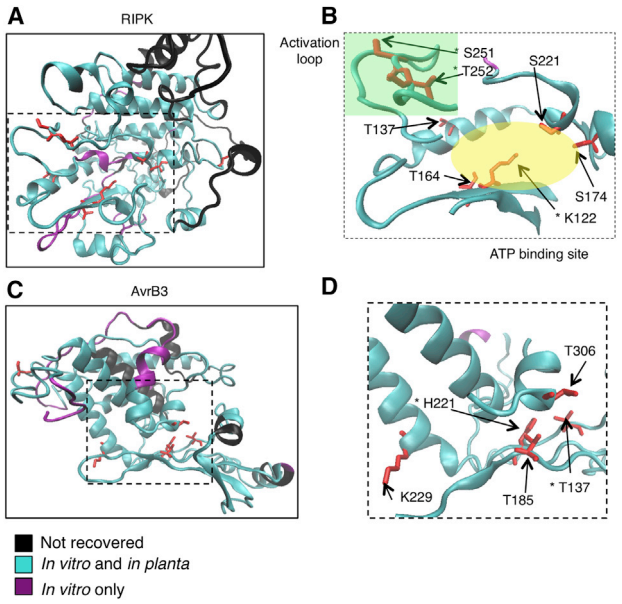

Figure 4. Acetylation Sites in Predicted 3D Structural Model of RIPK and AvrB3

In models generated by iTASSER, mass spectral coverage is indicated by color; cyan amino acids were seen in both in vitro and in planta experiments, purple amino acids were only recovered in in vitro samples, and black amino acids were not recovered. Unmodified versions of residues that were acetylated are shown as licorice versions in red. Functional analysis was performed with residues marked by asterisks.

(A and C) Full protein models are shown for RIPK (A) and AvrB3 (C). The dashed boxes indicate the area of the protein most acetylated in a HopZ3-dependent manner.

(B and D) RIPK (B) and AvrB3 (D) are magnified from the dashed boxes in (A) and (C). The protein in the foreground and background has been clipped to provide a clearer view of the structural proximity of the residues targeted for modification by HopZ3. In (B), shaded areas denote the ATP-binding site (yellow) and the activation loop (green). K122 is a conserved Lys that coordinates the γ-phosphate of ATP upon nucleotide binding.

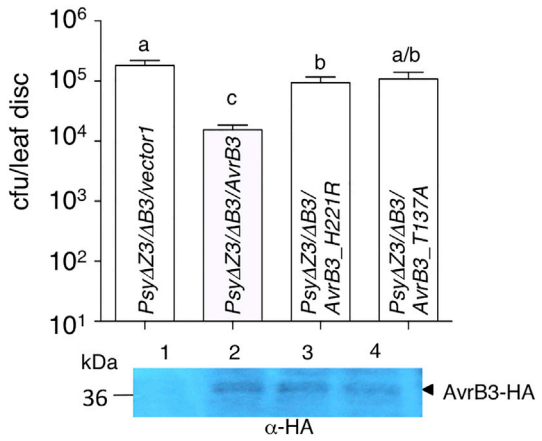

Figure 5. The Acetylation Sites of AvrB3 Are Important for Inducing Immunity

H221 and T137 are required for AvrB3-mediated immunity during infection. The bacterial population of *PsyΔavrB3ΔhopZ3* expressing AvrB3 was different than strains expressing mutated AvrB3 3 dpi in Col (ANOVA/Fisher's LSD; n = 36). (Lower panel) Expression of AvrB3-HA variants in *PsyΔavrB3ΔhopZ3* grown in KB medium (similar to the conditions before inoculation) was analyzed by immunoblotting. 1, empty vector (vector1); 2, AvrB3-HA; 3, AvrB3_H221R-HA; 4, AvrB3_T137A-HA.

radiolabeled phosphate from ATP (Figure 6A). LC-MS/MS analysis of phosphopeptides after in vitro kinase reactions with RIPK and HopZ3 confirmed that HopZ3 was also an RIPK substrate (Figure S5).

According to our structural/homology model, the K122 and S251/T252 residues that were modified by HopZ3-mediated acetylation in RIPK are in the ATP-binding pocket and in the activation loop, respectively (Figure 4B). To assess whether these residues are functionally important, we used site-directed mutagenesis and in vitro modification assays. Mutation of either K122 or S251/T252 reduced the ability of RIPK to phosphorylate itself as well as RIN4 (Figure 6C). The K122R and S251A/T252A variants of RIPK showed greatly reduced acetylation by HopZ3 (Figure 6D). When *ripk* mutant plants were infected, *PsyΔhopZ3* grew to the same level whether or not HopZ3 was added back, consistent with RIPK being targeted by HopZ3 (Figure 6E).

We next tested whether acetylation of RIN4 by HopZ3 can alter its ability to be phosphorylated by RIPK. To assess this, RIN4 was acetylated by HopZ3 in vitro and then added to RIPK in the presence of radiolabelled ATP. Acetylation of RIN4 by HopZ3 reduced the ability of RIN4 to be phosphorylated by RIPK in vitro (Figure 6F). In addition, when *rin4* mutant plants were infected, *PsyΔhopZ3* grew to the same level whether it was complemented with HopZ3 or not (Figure 6G). Together, our data indicate that HopZ3 can interfere with a key activating event, phosphorylation of RIN4, by inhibiting the kinase activity of RIPK and/or blocking the ability of RIN4 to be phosphorylated.

HopZ3 Suppresses RIN4 Phosphorylation Triggered by AvrB3/AvrRpm1$_{Psy}$ during Infection

Induction of RIN4-pT166 is needed for RPM1 activation during infection with *Pto*DC3000/AvrB or *Pto*DC3000/AvrRpm1 (Zhang et al., 2010). If HopZ3 suppresses activation of RPM1, RIN4-pT166 accumulation should be reduced during *Psy*B728a infection. To test this, we studied whether RIN4-pT166 occurred during infection with *Psy*B728a and its dependence on different effectors. *Psy*B728a modestly activated RIN4-pT166 accumulation. Importantly, deletion of HopZ3 resulted in increased RIN4-pT166 levels (Figure 6H), which correlated with suppression of bacterial growth (Figure 1C). As expected, this accumulation was largely due to AvrB3 and AvrRpm1$_{Psy}$, since *PsyΔhopZ3ΔavrB3ΔavrRpm1*$_{Psy}$ showed reduced RIN4-pT166 levels relative to that induced by *PsyΔhopZ3* (Figure 6H). Thus, HopZ3 suppressed the key signal activation step for RPM1 immunity, phosphorylation of RIN4 on T166.

DISCUSSION

This study established that acetylation on functionally important Lys, Ser, Thr, and/or His residues by HopZ3 can reduce the activity of an effector-immune complex. For the immune-stimulating AvrB3 effector, HopZ3 can acetylate sites critical for interactions with RIN4. For RIPK, HopZ3 can acetylate the

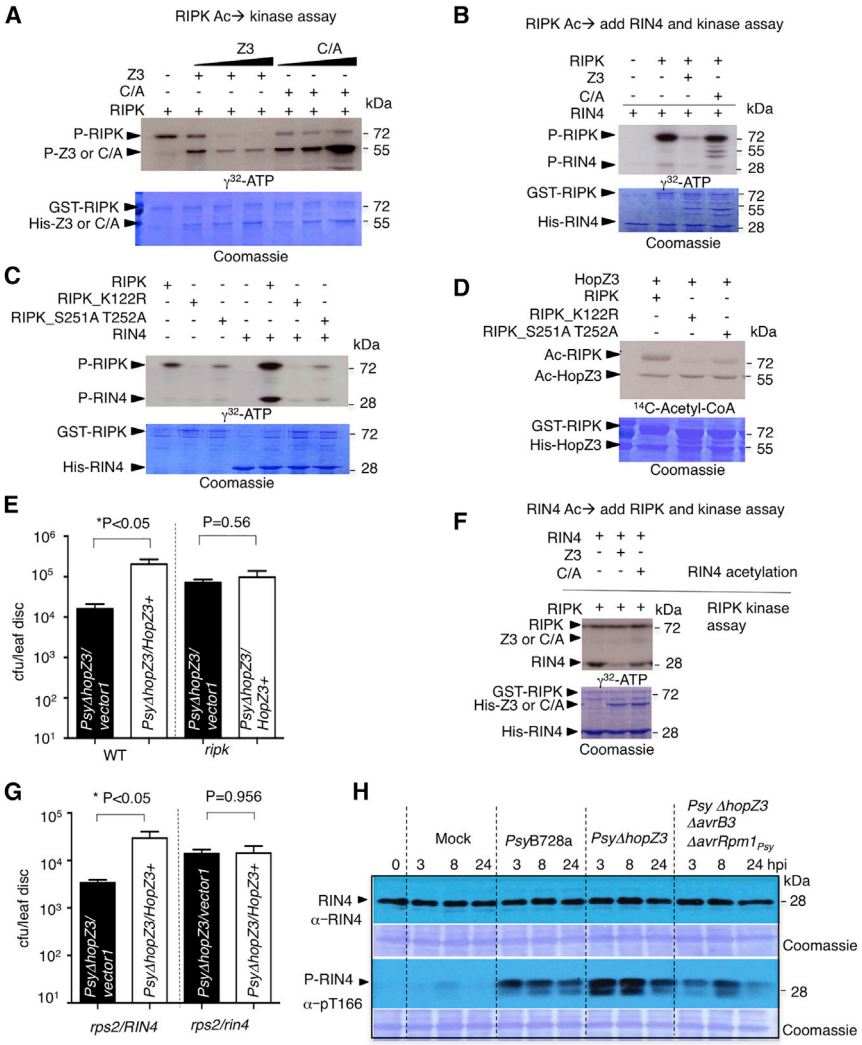

Figure 6. Acetylation of RIPK Affects Its Activity

(A) Acetylated RIPK shows reduced autophosphorylation. GST-RIPK bound to GSH-agarose was incubated with an increasing amount of His-HopZ3 (Z3) or His-HopZ3_C300A (C/A) in the presence of acetyl-CoA and IP_6. Subsequently, RIPK autophosphorylation was initiated by adding [γ-^{32}ATP] and detected by autoradiography. HopZ3 reduced RIPK autophosphorylation and transphosphorylation of HopZ3 by RIPK.

(B) Acetylated RIPK reduced transphosphorylation of RIN4.

(C) K122 and S251/T252 in RIPK are required for full kinase activity. GST-RIPK phosphorylates itself and RIN4, whereas GST-RIPK mutants show reduced activity. Proteins were separated by SDS-PAGE, stained with Coomassie blue (bottom), and subjected to autoradiography (top).

(D) Acetylation of RIPK mutants by HopZ3 is reduced. Acetylated proteins were detected by autoradiography.

(E) HopZ3 suppresses RIPK-mediated immunity. Populations of *Psy*Δ*hopZ3* with or without HopZ3 were not different in *ripk* plants 3 dpi.

(F) Acetylation of RIN4 prevents its phosphorylation by RIPK. Acetylated RIN4 is less efficiently phosphorylated by RIPK. RIN4 bound to Ni-NTA-agarose was acetylated by HopZ3, washed, and then incubated with RIPK and [γ-^{32}ATP].

(G) HopZ3 suppresses RIN4-mediated immunity. The growth of *Psy*Δ*hopZ3* with or without HopZ3 was significantly different in *rps2* RIN4, but not in *rps2 rin4* 3 dpi. (*rps2* was used to avoid the deleterious effect of *rin4*).

(H) HopZ3 blocks RIN4 phosphorylation during infection. *Psy*B728a, *Psy*Δ*hopZ3*, and *Psy* Δ*hopZ3*Δ*avrB3*Δ*avrRpm1*$_{Psy}$ were infiltrated at OD_{600} = 0.1 into leaves of Col (WT) and samples were collected at the indicated hours post-infection (hpi); 10 mM $MgSO_4$ (Mock) treatments were used as negative controls. Immunoblots were performed with either anti-RIN4 or anti-phospho-RIN4 T166 (pT166) antibodies. See also Figure S5.

nucleotide-binding site and activation loop to reduce kinase activity. Finally, for RIN4, HopZ3-mediated acetylation can reduce RIN4's ability to be phosphorylated by RIPK, a necessary step in activation of RPM1 signaling.

Our data suggest that targeting multiple members of a major effector-immune complex could be an effective way for HopZ3 to inactivate the complex and suppress defense signaling. By partially reducing the activity of multiple components, the outcome can be selected to accommodate conflicting requirements for maintaining virulence functions of effectors while reducing their defense-inducing recognition by plants. To elaborate this hypothesis, it is necessary to determine which specific acetylation and other PTMs occur in effector-immune complexes during infection. This requires technical advances to scale up purification of protein complexes for analysis by mass spectrometry (MS) and/or development of new reagents to detect specific acetylated residues of whole proteins of interest.

Interestingly, *P. syringae* strains other than *Psy*B728a also harbor alleles of HopZ3, AvrB, and AvrRpm1 or other effectors whose defense-inducing activities can be suppressed by HopZ3 (Table S4). These strains also may use a similar mechanism to that described in this work. Our finding that effector-effector interactions may contribute to reduced defense activation adds to the range of strategies in which effectors are deployed by pathogens to ameliorate the detection of other effectors.

Surprisingly, in the context of infection with *Psy*Δ*hopZ3*, both AvrB3 and AvrRpm1$_{Psy}$ are needed to activate immunity. Since these effectors interact in planta, they may act cooperatively, possibly by stabilizing each other, to activate the immune complex. We do not know of another example of a physically interacting effector pair in *P. syringae* where both effectors are simultaneously needed to stimulate the same immune pathway. The closest similarity may be AvrPto and AvrPtoB, which contribute additively to immune activation in tomato through

interaction with protein complexes that involve the immune regulator Prf (Lin and Martin, 2005).

Our study demonstrates that HopZ3 functionally interferes with the immune-activating properties of both AvrB3 and AvrRpm1$_{Psy}$. Although there are other examples of effector epistasis (Jamir et al., 2004; Szczesny et al., 2010; Tamaki et al., 1988; Tsiamis et al., 2000), this work implicates a plausible mechanism wherein one effector may directly modify others. Additional effector enzymes (Feng et al., 2012; Mackey et al., 2003; Rosebrock et al., 2007; Wang et al., 2010) may similarly modify both plant proteins and pathogen effectors.

We found that two HopZ3 *Arabidopsis* transgenic plant lines suppress immune activation by AvrB and AvrRpm1, as measured by changes in pathogen growth after low-dose infections. In contrast, a similar plant line expressing HopZ3 was unable to interfere with immunity-associated cell death induced by several effectors during high-dose infections (Lewis et al., 2014). Pathogen growth can sometimes be uncoupled from macroscopic symptoms, which may explain the different results obtained.

Effector-effector interactions are an understudied and often overlooked virulence strategy. It seems possible that bacterial effectors may form multi-protein complexes (such as HopZ3/AvrB3/AvrRpm1$_{Psy}$) to better target host components. Such interactions might allow whole effector complexes to form stable interactions with plant proteins inside plant cells, while reducing detectability by plant defense systems. Something similar to this is seen in the human pathogen *Chlamydia trachomatis*, where two type III Inc effectors interact and co-localize with Src family kinases in the membrane that surrounds the vacuolar compartment in which the pathogen resides (Mital et al., 2010). The observation that AvrB3 can affect the localization of HopZ3 is consistent with these findings.

This study documented a new stable acetylation modification on a key His residue in addition to the established YopJ family acetylation modifications on Lys, Ser, and Thr residues (Mukherjee et al., 2006; Trosky et al., 2007). His acetylations have not been widely reported in any system. A kinase substrate of YopJ may have a His modification, but its dependence on YopJ catalytic activity has yet to be validated (Paquette et al., 2012). Previous work using nuclear magnetic resonance (NMR) showed that a chemically induced acetylation of a Lys residue in ubiquitin occurred via an unstable acetylated His intermediate (Macdonald et al., 2000). Therefore, it seems possible that some acetyltransferase-mediated His acetylations may be unstable and, thus, could have been missed in previous analyses. Our finding of a His acetylation modification in AvrB3 suggests that His modifications should be examined carefully in other acetyltransferase substrates.

In addition to suppressing AvrB3/AvrRpm1$_{Psy}$-triggered immunity (this study), HopZ3 suppresses flg22 responses (Lewis et al., 2014). Interestingly, HopZ3 interacts with and/or acetylates RLCK family members (BIK1 and PBL1) with known roles in flg22 signaling. How acetylation mechanistically blocks flg22 response proteins will be an interesting area for future studies.

We found two examples of HopZ3-mediated acetylation that overlap with identified phosphorylation sites in RIN4, S47 and T160 (Chung et al., 2014; Liu et al., 2011; Nühse et al., 2004, 2007). Although these sites individually have no known biological function, competitive PTM of S47 and T160 possibly together with other modifications in RIN4 during infection might control RIN4 function. *Xanthomonas* AvrAC modifies the same sites as HopZ3 in RIPK (S251 and T252) within the activation loop (Feng et al., 2012). In the case of AvrAC, the modification involves the addition of uridine 5-monophosphate. Whether AvrAC also modifies other members of the RPM1 immune complex or other effectors remains to be investigated.

In summary, this work established that an effector-immune complex can be modified and inactivated by acetylation. This explains why loss of the HopZ3 effector from *Psy*B728a causes greatly reduced pathogen growth on *Arabidopsis* genotypes that have a functional RPM1 pathway. Interestingly, HopZ3-mediated acetylation may affect effector-immune complex components through multiple mechanisms by (1) inactivating a kinase, (2) modifying protein-protein interaction sites needed for signal activation, and (3) preventing other PTMs.

EXPERIMENTAL PROCEDURES

All genes were amplified by PCR using primers that incorporated a specific restriction enzyme site or att domain (Table S7). All PCR products were transferred into the pDONR207 following the Gateway manual using the BP clonase enzyme mix (Invitrogen) and were sequence validated. To clone into pENTR vectors, genes were recombined into nYFP (pG005, The European *Arabidopsis* Stock Centre), cYFP (pG006, The European *Arabidopsis* Stock Centre), pLaw10 (which contained Gal4 DNA-binding domain), and pLaw11 (which contained the Gal4 activation domain) using the LR clonase enzyme mix, according to the manufacturer's instructions (Invitrogen). The site-directed mutagenesis was generated by PCR using overlapping primers incorporating the mutation of interest (Table S5). Point mutants were cloned into either a pET28a or pGEX 4T-3 TEV vector and sequenced to ensure that no additional mutations were introduced.

Strains and Plasmids

Bacteria strains and plasmids are listed in Tables S5 and S6.

Protein Production and Purification

To purify GST and His fusion proteins, *E. coli* BL21 (DE) cells transformed with GST or His-tagged constructs were induced at an optical density 600 (OD_{600}) of 0.6–0.8 with 0.2 mM isopropyl-β-δ-thiogalactopyranoside for 2–5 hr at 30°C. Cellular extracts were made by sonication and clarified at 10,000 × *g* for 20 min. GST fusion proteins were purified by binding to glutathione-conjugated beads and eluted with reduced glutathione (GE Healthcare). His fusion proteins were purified by binding to Ni-NTA agarose beads (QIAGEN) and then eluted with 300 mM imidazole.

Plant Lines and Growth Conditions

Plant growth chamber conditions were as described previously (Lu et al., 2003). Dexamethasone-inducible constructs encoding HopZ3-HA:pBAV154 (Lee et al., 2012b) were transformed into *Agrobacterium GV3101*. Transgenic Col-0 *Arabidopsis* plants were generated by a floral dip transformation procedure (Bent, 2006). All other *Arabidopsis* lines (*rps2*, *rps2rin4*, *ripk*, and *rpm1*) were described previously (Belkhadir et al., 2004; Liu et al., 2011; Mackey et al., 2002). *Nicotiana benthamiana* was used for transient expression studies as described previously (Lee et al., 2012b).

Generation of Mutant Bacteria and Complementation Constructs

Strains bearing deletions of AvrB3 and/or AvrRpm1$_{Psy}$ were constructed using sacB-mediated negative selection as described previously (Vinatzer et al., 2006), except that the pMTN1907 vector was used (Baltrus et al., 2012). Mutants were confirmed by PCR amplification of the deletion. To complement the mutant phenotype, the WT AvrB3 and AvrRpm1$_{Psy}$ were cloned into

pBAV226 (Vinatzer et al., 2006). This construct was then introduced into the *Psy*Δ*hopZ3* Δ*avrB3* or *Psy*Δ*hopZ3* Δ*avrRpm1*$_{Psy}$ double-mutant strains by electroporation.

Bacterial Growth Assays

Overnight cultures of *P. syringae* were diluted 1:10 and grown for 3 hr at 30°C. The bacteria (OD_{600} = 0.0001 or 0.0003 for *Pto*DC3000 and 0.0003 for *Psy*B728a derivatives) were syringe infiltrated into at least 8–28 leaves of *Arabidopsis* plants (21–24 days old). To measure epiphytic growth, *Arabidopsis* plants were sprayed with *Psy*B728a derivatives at an OD_{600} = 0.03 (in 10 mM $MgSO_4$ without additives) and covered with a dome without holes for 3 days. For evaluation of bacterial growth, eight 1-cm^2-diameter leaf disks for each strain were either homogenized by mechanical disruption or vortexed to collect epiphytic bacteria in 200 μl of 10 mM $MgSO_4$. Samples were serially diluted and enumerated by counting colony-forming units after plating on LB agar containing antibiotics. All experiments were repeated two to three times with similar results.

Acetylation Assays

In vitro acetylation assays using radiolabel were performed as previously described (Jiang et al., 2013; Lewis et al., 2013). Purified substrates (1–3 μg) and 1 μg purified His-HopZ3 or His-HopZ3_C300A were mixed with acetylation reaction mixture containing 50 mM HEPES (pH 8.0), 10% glycerol, 5 μM IP_6, and 1–2 μl ^{14}C-Acetyl-CoA (56 μCi/μM) (PerkinElmer) in a total volume of 20 μl. All acetylation reactions were incubated at room temperature (RT) for 2–3 hr and terminated by the addition of SDS-PAGE loading buffer and boiling for 5 min. Proteins were separated by SDS-PAGE. After electrophoresis, gels were dried on 3M paper and exposed to X-ray film for 3–14 days. Each data point consisted of at least two replicates. Heavy isotope in vitro as well as in vivo acetylation assays for LC-MS/MS-based mapping are provided in the Supplemental Experimental Procedures.

In Vitro Kinase Assay

For RIPK auto- and transphosphorylation assays, 0.5 μg GST-RIPK, GST-RIPK (T251A/T252A), and GST-RIPK (K122R) proteins and 3 μg RIN4 were incubated with phosphorylation mix (10 mM $MgSO_4$, 10 μM ATP, and 10 μM γ− [^{32}P]-ATP) for 30 min at RT. To evaluate the influence of acetylation on RIPK kinase activity, reactions of protein bound to glutathione beads were performed. Bead-bound GST-RIPK (0.5 μg) and the purified His-HopZ3 (0.25, 0.5, and 1 μg) or His-HopZ3_C300A (0.25, 0.5, and 1 μg) were first incubated in acetylation reaction mixture (50 mM HEPES [pH 8.0], 10% glycerol, 5 μM IP_6, and 50 μM acetyl-CoA; Sigma) for 2 hr at RT or 16 hr in a cold room (~4°C). After washing the beads with the washing buffer (50 mM HEPES [pH 8.0], 50 mM NaCl, and 10% glycerol), the phosphorylation reaction was initiated by adding phosphorylation mix (10 mM $MgSO_4$, 10 μM ATP, and 10 μM γ− [^{32}P]-ATP; PerkinElmer) for 30 min at RT. To determine the level of RIN4 phosphorylation by RIPK after acetylation by HopZ3, bead-bound His-RIN4 (3 μg) was incubated with His-HopZ3 (1 μg) and His-HopZ3_C300A (1 μg) in acetylation reaction mixture for 2 hr at RT. After washing the beads twice, the phosphorylation reaction was initiated by adding 0.5 μg RIPK with the phosphorylation mix for 30 min at RT. All reactions were terminated by adding Laemmli buffer and boiling for 5 min. Proteins were separated by 12% SDS-PAGE and signals were visualized by X-ray film exposure for 16 hr. All experiments were repeated two to three times with similar results.

BIFC Assay

Constructs and vectors used in this work are listed in Table S6. Each test protein coding sequence was cloned into either the pG005 vector, which fused the N-terminal half of YFP (nYFP, 1–155 amino acid [aa]) to the C terminus of the protein, or was cloned into the pG006 vector, which fused the C-terminal half of YFP (cYFP, 156–239 aa) to the C terminus of the protein. Binary plasmids with a helper pSoup were transformed into *A. tumefaciens* GV3101 by electroporation. Co-infiltration of Agrobacteria containing the BIFC constructs into *N. benthamiana* leaves was done at a final concentration of OD_{600} = 0.8. Epidermal cells of *N. benthamiana* leaves were assayed for fluorescence 48 hr after agroinfiltration. YFP fluorescence (visible only when proteins fused to YFP halves interact) was visualized using a Zeiss LSM710 confocal laser-scanning microscope by excitation with a single line 488-nm laser, and emission was collected with filter set to 489–573 nm. All experiments were repeated two times with similar results.

Subcellular Fractionation

A. tumefaciens strain C58C1 bacteria carrying pBAV150-HopZ3 and pBAV154-AvrB3 or AvrB3_G2A binary vector, respectively, were transiently co-infiltrated into *N. benthamiana* leaves (Lee et al., 2012b). Two days after the infiltration of Agrobacteria, expression of transgenes was induced by spraying 30 μM dexamethasone on the plant leaves. After 16 hr, leaf samples were harvested for subcellular fractionation and immunoblotting as described in a previous report (Lu et al., 2003). Briefly, samples were ground with grinding buffer (50 mM Tris-HCl [pH 7.5], 0.33 M sucrose, 5 mM EDTA, and 1 mM DTT; Roche) and then centrifuged at 10,000 × *g* at 4°C to pellet insoluble material. Supernatant was ultracentrifuged at 100,000 × *g* at 4°C for 1 hr to precipitate total membrane fraction. After partitioning, the supernatant and the pellet were used as soluble and membrane fractions, respectively. After separation by SDS-PAGE and transfer to PVDF membranes, proteins were probed with anti-GFP (Covance), anti-HA (Covance, 1:1,000), anti-H^+-ATPase (Agrisera, 1:7,500), and anti-cFBP (Agrisera, 1:20,000) antibodies. The experiment was repeated two times with similar results.

Yeast Two-Hybrid Assay

Yeast two-hybrid assays were analyzed based on the requirement of His for yeast growth and expression of the *lacZ* gene reporter (Cantu et al., 2013). More detailed methods are provided in the Supplemental Experimental Procedures.

Immunoblotting Assay

For HopZ3-GFP immmunoprecipitation, pBAV150-derived constructs with HopZ3 or pBAV150-HopZ3_C300A were used to transiently express proteins in *N. benthamiana* after agroinfection. Plants were treated with 30 μM dexamethasone for 16 hr to induce HopZ3-GFP expression. Proteins were extracted with lysis buffer (50 mM Tris [pH 7.5], 50 mM NaCl, 1 mM EDTA, 1 mM DTT, and 0.2% Triton X-100) containing protease inhibitor (Roche), phosphatase inhibitor (Thermo Scientific), and 3 μM TrichostatinA (Sigma). Clarified total protein lysate was incubated for 3 hr with antibody directed against full-length GFP (Clontech Laboratories) at 4°C followed by incubation for 1 hr with 30 μl fast-flow protein A agarose beads (Roche). After washing the beads three times with the lysis buffer, proteins were eluted by boiling with Laemmli loading buffer. Samples were analyzed by western blotting with anti-GFP (1:5,000) and anti-acetylated Lys (1:1,000) antibody (Cell Signaling Technology).

For detecting RIN4 phosphorylation in *Arabidopsis*, 21–24 old plants were infiltrated with *Pto*DC3000- and *Psy*B728a-derived strains at OD_{600} = 0.1. Leaf tissue was collected 6, 18, and 24 hr after infections for protein analysis. *Arabidopsis* leaves were ground in liquid nitrogen and resuspended in lysis buffer including phosphatase inhibitor (Roche). The resulting samples were analyzed by western blotting and probed with anti-pRIN4 (1:1,000, a gift from Dr. Gitta Coaker at University of California, Davis) and anti-RIN4 (1:5,000, a gift from Dr. Gitta Coaker) antibodies (Liu et al., 2011). The experiment was repeated two times with similar results.

Structural Modeling

To assess the relevance of the acetylated residues found by MS, we modeled the structure of the HopZ3 substrates using the Iterative Threading Assembly Refinement (iTASSER) structural prediction software (Roy et al., 2010; Yang et al., 2015; Zhang, 2008). The top models were assessed for the best possible model based on confidence score (C-score) calculated based on the significance of threading to the template alignments and convergence to the parameters of the structural assembly simulations (Roy et al., 2010; Yang et al., 2015; Zhang, 2008). Model visualizations were generated using VMD 1.9.1, using the new cartoon setting coloring by MS coverage as indicated in the figure legend. Acetylation sites were labeled

using the licorice setting and coloring red; however, the sites shown are not acetylated in the model.

LC-MS/MS Analysis

MS was performed at the Medical Genome Facility Proteomics Core at Mayo Clinic. Additional (more detailed) methods are provided in the Supplemental Experimental Procedures.

ACCESSION NUMBERS

The MS data have been deposited in ProteomeCentral (http://proteomecentral.proteomexchange.org) via the PRIDE partner repository with the dataset identifier ProteomeXchange Consortium: PXD001344.

SUPPLEMENTAL INFORMATION

Supplemental Information includes Supplemental Experimental Procedures, five figures, seven tables, and amino acid sequence alignments and can be found with this article online at http://dx.doi.org/10.1016/j.celrep.2015.10.029.

AUTHOR CONTRIBUTIONS

J.L., J.J., R.W.M., S.J.K., and J.T.G. designed experiments. J.L., D.W., A.J.M., and K.A.C. performed experiments. J.L., A.J.M., D.W., J.J., H.X., and S.M.F. analyzed data. J.L., D.W., and J.T.G. wrote the paper with input from A.J.M., J.J., S.J.K., and R.W.M.

ACKNOWLEDGMENTS

This work was funded by National Science Foundation (NSF) grants IOS0822393 and IOS1238201. We thank D. Mackey, J.L. Dangl, K. Orth, and G. Coaker for reagents; H. Hang and T. Wroblewski for useful discussions; and H.W. Jung for the *Arabidopsis* and *N. benthamiana* prey libraries used for the genome-wide yeast two-hybrid screen.

Received: September 8, 2014
Revised: September 10, 2015
Accepted: October 9, 2015
Published: November 12, 2015

REFERENCES

Andreasson, E., Jenkins, T., Brodersen, P., Thorgrimsen, S., Petersen, N.H., Zhu, S., Qiu, J.L., Micheelsen, P., Rocher, A., Petersen, M., et al. (2005). The MAP kinase substrate MKS1 is a regulator of plant defense responses. EMBO J. *24*, 2579–2589.

Asai, T., Tena, G., Plotnikova, J., Willmann, M.R., Chiu, W.L., Gomez-Gomez, L., Boller, T., Ausubel, F.M., and Sheen, J. (2002). MAP kinase signalling cascade in *Arabidopsis* innate immunity. Nature *415*, 977–983.

Baltrus, D.A., Nishimura, M.T., Dougherty, K.M., Biswas, S., Mukhtar, M.S., Vicente, J., Holub, E.B., and Dangl, J.L. (2012). The molecular basis of host specialization in bean pathovars of *Pseudomonas syringae*. Mol. Plant Microbe Interact. *25*, 877–888.

Belkhadir, Y., Nimchuk, Z., Hubert, D.A., Mackey, D., and Dangl, J.L. (2004). *Arabidopsis* RIN4 negatively regulates disease resistance mediated by RPS2 and RPM1 downstream or independent of the NDR1 signal modulator and is not required for the virulence functions of bacterial type III effectors AvrRpt2 or AvrRpm1. Plant Cell *16*, 2822–2835.

Bent, A. (2006). *Arabidopsis thaliana* floral dip transformation method. Methods Mol. Biol. *343*, 87–103.

Bent, A.F., Kunkel, B.N., Dahlbeck, D., Brown, K.L., Schmidt, R., Giraudat, J., Leung, J., and Staskawicz, B.J. (1994). RPS2 of *Arabidopsis thaliana*: a leucine-rich repeat class of plant disease resistance genes. Science *265*, 1856–1860.

Bisgrove, S.R., Simonich, M.T., Smith, N.M., Sattler, A., and Innes, R.W. (1994). A disease resistance gene in *Arabidopsis* with specificity for two different pathogen avirulence genes. Plant Cell *6*, 927–933.

Cantu, D., Yang, B., Ruan, R., Li, K., Menzo, V., Fu, D., Chern, M., Ronald, P.C., and Dubcovsky, J. (2013). Comparative analysis of protein-protein interactions in the defense response of rice and wheat. BMC Genomics *14*, 166.

Cheong, M.S., Kirik, A., Kim, J.G., Frame, K., Kirik, V., and Mudgett, M.B. (2014). AvrBsT acetylates *Arabidopsis* ACIP1, a protein that associates with microtubules and is required for immunity. PLoS Pathog. *10*, e1003952.

Chisholm, S.T., Coaker, G., Day, B., and Staskawicz, B.J. (2006). Host-microbe interactions: shaping the evolution of the plant immune response. Cell *124*, 803–814.

Chung, E.H., El-Kasmi, F., He, Y., Loehr, A., and Dangl, J.L. (2014). A plant phosphoswitch platform repeatedly targeted by type III effector proteins regulates the output of both tiers of plant immune receptors. Cell Host Microbe *16*, 484–494.

Cui, H., Wang, Y., Xue, L., Chu, J., Yan, C., Fu, J., Chen, M., Innes, R.W., and Zhou, J.M. (2010). *Pseudomonas syringae* effector protein AvrB perturbs *Arabidopsis* hormone signaling by activating MAP kinase 4. Cell Host Microbe *7*, 164–175.

Deribe, Y.L., Pawson, T., and Dikic, I. (2010). Post-translational modifications in signal integration. Nat. Struct. Mol. Biol. *17*, 666–672.

Deslandes, L., and Rivas, S. (2012). Catch me if you can: bacterial effectors and plant targets. Trends Plant Sci. *17*, 644–655.

Desveaux, D., Singer, A.U., Wu, A.J., McNulty, B.C., Musselwhite, L., Nimchuk, Z., Sondek, J., and Dangl, J.L. (2007). Type III effector activation via nucleotide binding, phosphorylation, and host target interaction. PLoS Pathog. *3*, e48.

Ellis, J., and Dodds, P. (2003). Plant pathology: monitoring a pathogen-targeted host protein. Curr. Biol. *13*, R400–R402.

Feng, F., Yang, F., Rong, W., Wu, X., Zhang, J., Chen, S., He, C., and Zhou, J.M. (2012). A *Xanthomonas* uridine 5′-monophosphate transferase inhibits plant immune kinases. Nature *485*, 114–118.

Gabriel, D.W., Burges, A., and Lazo, G.R. (1986). Gene-for-gene interactions of five cloned avirulence genes from *Xanthomonas campestris* pv. *malvacearum* with specific resistance genes in cotton. Proc. Natl. Acad. Sci. USA *83*, 6415–6419.

Gassmann, M., Grenacher, B., Rohde, B., and Vogel, J. (2009). Quantifying Western blots: pitfalls of densitometry. Electrophoresis *30*, 1845–1855.

Grant, M.R., Godiard, L., Straube, E., Ashfield, T., Lewald, J., Sattler, A., Innes, R.W., and Dangl, J.L. (1995). Structure of the *Arabidopsis RPM1* gene enabling dual specificity disease resistance. Science *269*, 843–846.

Guo, M., Tian, F., Wamboldt, Y., and Alfano, J.R. (2009). The majority of the type III effector inventory of *Pseudomonas syringae* pv. *tomato* DC3000 can suppress plant immunity. Mol. Plant Microbe Interact. *22*, 1069–1080.

Hirano, S.S., Charkowski, A.O., Collmer, A., Willis, D.K., and Upper, C.D. (1999). Role of the Hrp type III protein secretion system in growth of *Pseudomonas syringae* pv. *syringae* B728a on host plants in the field. Proc. Natl. Acad. Sci. USA *96*, 9851–9856.

Jamir, Y., Guo, M., Oh, H.S., Petnicki-Ocwieja, T., Chen, S., Tang, X., Dickman, M.B., Collmer, A., and Alfano, J.R. (2004). Identification of *Pseudomonas syringae* type III effectors that can suppress programmed cell death in plants and yeast. Plant J. *37*, 554–565.

Jiang, S., Yao, J., Ma, K.W., Zhou, H., Song, J., He, S.Y., and Ma, W. (2013). Bacterial effector activates jasmonate signaling by directly targeting JAZ transcriptional repressors. PLoS Pathog. *9*, e1003715.

Jones, J.D., and Dangl, J.L. (2006). The plant immune system. Nature *444*, 323–329.

Karve, T.M., and Cheema, A.K. (2011). Small changes huge impact: the role of protein posttranslational modifications in cellular homeostasis and disease. J. Amino Acids *2011*, 207691.

Kim, H.S., Desveaux, D., Singer, A.U., Patel, P., Sondek, J., and Dangl, J.L. (2005). The Pseudomonas syringae effector AvrRpt2 cleaves its C-terminally acylated target, RIN4, from *Arabidopsis* membranes to block RPM1 activation. Proc. Natl. Acad. Sci. USA *102*, 6496–6501.

Le Roux, C., Huet, G., Jauneau, A., Camborde, L., Trémousaygue, D., Kraut, A., Zhou, B., Levaillant, M., Adachi, H., Yoshioka, H., et al. (2015). A receptor pair with an integrated decoy converts pathogen disabling of transcription factors to immunity. Cell *161*, 1074–1088.

Lee, A.H., Hurley, B., Felsensteiner, C., Yea, C., Ckurshumova, W., Bartetzko, V., Wang, P.W., Quach, V., Lewis, J.D., Liu, Y.C., et al. (2012a). A bacterial acetyltransferase destroys plant microtubule networks and blocks secretion. PLoS Pathog. *8*, e1002523.

Lee, J., Teitzel, G.M., Munkvold, K., del Pozo, O., Martin, G.B., Michelmore, R.W., and Greenberg, J.T. (2012b). Type III secretion and effectors shape the survival and growth pattern of *Pseudomonas syringae* on leaf surfaces. Plant Physiol. *158*, 1803–1818.

Lewis, J.D., Abada, W., Ma, W., Guttman, D.S., and Desveaux, D. (2008). The HopZ family of *Pseudomonas syringae* type III effectors require myristoylation for virulence and avirulence functions in *Arabidopsis thaliana*. J. Bacteriol. *190*, 2880–2891.

Lewis, J.D., Lee, A., Ma, W., Zhou, H., Guttman, D.S., and Desveaux, D. (2011). The YopJ superfamily in plant-associated bacteria. Mol. Plant Pathol. *12*, 928–937.

Lewis, J.D., Lee, A.H., Hassan, J.A., Wan, J., Hurley, B., Jhingree, J.R., Wang, P.W., Lo, T., Youn, J.Y., Guttman, D.S., and Desveaux, D. (2013). The *Arabidopsis* ZED1 pseudokinase is required for ZAR1-mediated immunity induced by the *Pseudomonas syringae* type III effector HopZ1a. Proc. Natl. Acad. Sci. USA *110*, 18722–18727.

Lewis, J.D., Wilton, M., Mott, G.A., Lu, W., Hassan, J.A., Guttman, D.S., and Desveaux, D. (2014). Immunomodulation by the *Pseudomonas syringae* HopZ type III effector family in *Arabidopsis*. PLoS ONE *9*, e116152.

Lin, N.C., and Martin, G.B. (2005). An avrPto/avrPtoB mutant of *Pseudomonas syringae* pv. *tomato* DC3000 does not elicit Pto-mediated resistance and is less virulent on tomato. Mol. Plant Microbe Interact. *18*, 43–51.

Liu, J., Elmore, J.M., Lin, Z.J., and Coaker, G. (2011). A receptor-like cytoplasmic kinase phosphorylates the host target RIN4, leading to the activation of a plant innate immune receptor. Cell Host Microbe *9*, 137–146.

Lu, H., Rate, D.N., Song, J.T., and Greenberg, J.T. (2003). ACD6, a novel ankyrin protein, is a regulator and an effector of salicylic acid signaling in the *Arabidopsis* defense response. Plant Cell *15*, 2408–2420.

Ma, K.W., Jiang, S., Hawara, E., Lee, D., Pan, S., Coaker, G., Song, J., and Ma, W. (2015). Two serine residues in Pseudomonas syringae effector HopZ1a are required for acetyltransferase activity and association with the host co-factor. New Phytol. *208*, 1157–1168.

Macdonald, J.M., Haas, A.L., and London, R.E. (2000). Novel mechanism of surface catalysis of protein adduct formation. NMR studies of the acetylation of ubiquitin. J. Biol. Chem. *275*, 31908–31913.

Mackey, D., Holt, B.F., 3rd, Wiig, A., and Dangl, J.L. (2002). RIN4 interacts with Pseudomonas syringae type III effector molecules and is required for RPM1-mediated resistance in *Arabidopsis*. Cell *108*, 743–754.

Mackey, D., Belkhadir, Y., Alonso, J.M., Ecker, J.R., and Dangl, J.L. (2003). Arabidopsis RIN4 is a target of the type III virulence effector AvrRpt2 and modulates RPS2-mediated resistance. Cell *112*, 379–389.

Mital, J., Miller, N.J., Fischer, E.R., and Hackstadt, T. (2010). Specific *chlamydial* inclusion membrane proteins associate with active Src family kinases in microdomains that interact with the host microtubule network. Cell. Microbiol. *12*, 1235–1249.

Mittal, R., Peak-Chew, S.Y., Sade, R.S., Vallis, Y., and McMahon, H.T. (2010). The acetyltransferase activity of the bacterial toxin YopJ of *Yersinia* is activated by eukaryotic host cell inositol hexakisphosphate. J. Biol. Chem. *285*, 19927–19934.

Mucyn, T.S., Clemente, A., Andriotis, V.M., Balmuth, A.L., Oldroyd, G.E., Staskawicz, B.J., and Rathjen, J.P. (2006). The tomato NBARC-LRR protein Prf interacts with Pto kinase in vivo to regulate specific plant immunity. Plant Cell *18*, 2792–2806.

Mukherjee, S., Keitany, G., Li, Y., Wang, Y., Ball, H.L., Goldsmith, E.J., and Orth, K. (2006). *Yersinia* YopJ acetylates and inhibits kinase activation by blocking phosphorylation. Science *312*, 1211–1214.

Nimchuk, Z., Marois, E., Kjemtrup, S., Leister, R.T., Katagiri, F., and Dangl, J.L. (2000). Eukaryotic fatty acylation drives plasma membrane targeting and enhances function of several type III effector proteins from *Pseudomonas syringae*. Cell *101*, 353–363.

Nühse, T.S., Stensballe, A., Jensen, O.N., and Peck, S.C. (2004). Phosphoproteomics of the Arabidopsis plasma membrane and a new phosphorylation site database. Plant Cell *16*, 2394–2405.

Nühse, T.S., Bottrill, A.R., Jones, A.M., and Peck, S.C. (2007). Quantitative phosphoproteomic analysis of plasma membrane proteins reveals regulatory mechanisms of plant innate immune responses. Plant J. *51*, 931–940.

Oh, C.S., and Martin, G.B. (2011). Effector-triggered immunity mediated by the Pto kinase. Trends Plant Sci. *16*, 132–140.

Paquette, N., Conlon, J., Sweet, C., Rus, F., Wilson, L., Pereira, A., Rosadini, C.V., Goutagny, N., Weber, A.N., Lane, W.S., et al. (2012). Serine/threonine acetylation of TGFβ-activated kinase (TAK1) by Yersinia pestis YopJ inhibits innate immune signaling. Proc. Natl. Acad. Sci. USA *109*, 12710–12715.

Ritter, C., and Dangl, J.L. (1995). The avrRpm1 gene of *Pseudomonas syringae* pv. *maculicola* is required for virulence on Arabidopsis. Mol. Plant Microbe Interact. *8*, 444–453.

Rosebrock, T.R., Zeng, L., Brady, J.J., Abramovitch, R.B., Xiao, F., and Martin, G.B. (2007). A bacterial E3 ubiquitin ligase targets a host protein kinase to disrupt plant immunity. Nature *448*, 370–374.

Roy, A., Kucukural, A., and Zhang, Y. (2010). I-TASSER: a unified platform for automated protein structure and function prediction. Nat. Protoc. *5*, 725–738.

Salomon, D., and Orth, K. (2013). What pathogens have taught us about post-translational modifications. Cell Host Microbe *14*, 269–279.

Sarris, P.F., Duxbury, Z., Huh, S.U., Ma, Y., Segonzac, C., Sklenar, J., Derbyshire, P., Cevik, V., Rallapalli, G., Saucet, S.B., et al. (2015). A plant immune receptor detects pathogen effectors that target WRKY transcription factors. Cell *161*, 1089–1100.

Shen, H., and Keen, N.T. (1993). Characterization of the promoter of avirulence gene D from *Pseudomonas syringae* pv. *tomato*. J. Bacteriol. *175*, 5916–5924.

Simonich, M.T., and Innes, R.W. (1995). A disease resistance gene in Arabidopsis with specificity for the avrPph3 gene of *Pseudomonas syringae* pv. *phaseolicola*. Mol. Plant Microbe Interact. *8*, 637–640.

Staskawicz, B.J., Dahlbeck, D., and Keen, N.T. (1984). Cloned avirulence gene of *Pseudomonas syringae* pv. *glycinea* determines race-specific incompatibility on Glycine max (L.) Merr. Proc. Natl. Acad. Sci. USA *81*, 6024–6028.

Sun, X., Greenwood, D.R., Templeton, M.D., Libich, D.S., McGhie, T.K., Xue, B., Yoon, M., Cui, W., Kirk, C.A., Jones, W.T., et al. (2014). The intrinsically disordered structural platform of the plant defence hub protein RPM1-interacting protein 4 provides insights into its mode of action in the host-pathogen interface and evolution of the nitrate-induced domain protein family. FEBS J. *281*, 3955–3979.

Szczesny, R., Büttner, D., Escolar, L., Schulze, S., Seiferth, A., and Bonas, U. (2010). Suppression of the AvrBs1-specific hypersensitive response by the YopJ effector homolog AvrBsT from *Xanthomonas* depends on a SNF1-related kinase. New Phytol. *187*, 1058–1074.

Tamaki, S., Dahlbeck, D., Staskawicz, B., and Keen, N.T. (1988). Characterization and expression of two avirulence genes cloned from *Pseudomonas syringae* pv. *glycinea*. J. Bacteriol. *170*, 4846–4854.

Trosky, J.E., Li, Y., Mukherjee, S., Keitany, G., Ball, H., and Orth, K. (2007). VopA inhibits ATP binding by acetylating the catalytic loop of MAPK kinases. J. Biol. Chem. *282*, 34299–34305.

Tsiamis, G., Mansfield, J.W., Hockenhull, R., Jackson, R.W., Sesma, A., Athanassopoulos, E., Bennett, M.A., Stevens, C., Vivian, A., Taylor, J.D., and Murillo, J. (2000). Cultivar-specific avirulence and virulence functions assigned

to avrPphF in *Pseudomonas syringae* pv. *phaseolicola*, the cause of bean halo-blight disease. EMBO J. *19*, 3204–3214.

Vinatzer, B.A., Teitzel, G.M., Lee, M.W., Jelenska, J., Hotton, S., Fairfax, K., Jenrette, J., and Greenberg, J.T. (2006). The type III effector repertoire of *Pseudomonas syringae* pv. *syringae* B728a and its role in survival and disease on host and non-host plants. Mol. Microbiol. *62*, 26–44.

Walter, M., Chaban, C., Schütze, K., Batistic, O., Weckermann, K., Näke, C., Blazevic, D., Grefen, C., Schumacher, K., Oecking, C., et al. (2004). Visualization of protein interactions in living plant cells using bimolecular fluorescence complementation. Plant J. *40*, 428–438.

Wang, Y., Li, J., Hou, S., Wang, X., Li, Y., Ren, D., Chen, S., Tang, X., and Zhou, J.M. (2010). A *Pseudomonas syringae* ADP-ribosyltransferase inhibits *Arabidopsis* mitogen-activated protein kinase kinases. Plant Cell *22*, 2033–2044.

Whalen, M.C., Stall, R.E., and Staskawicz, B.J. (1988). Characterization of a gene from a tomato pathogen determining hypersensitive resistance in non-host species and genetic analysis of this resistance in bean. Proc. Natl. Acad. Sci. USA *85*, 6743–6747.

Wilton, M., Subramaniam, R., Elmore, J., Felsensteiner, C., Coaker, G., and Desveaux, D. (2010). The type III effector $HopF2_{Pto}$ targets *Arabidopsis* RIN4 protein to promote *Pseudomonas syringae* virulence. Proc. Natl. Acad. Sci. USA *107*, 2349–2354.

Yang, J., Yan, R., Roy, A., Xu, D., Poisson, J., and Zhang, Y. (2015). The I-TASSER Suite: protein structure and function prediction. Nat. Methods *12*, 7–8.

Zhang, Y. (2008). I-TASSER server for protein 3D structure prediction. BMC Bioinformatics *9*, 40.

Zhang, J., Li, W., Xiang, T., Liu, Z., Laluk, K., Ding, X., Zou, Y., Gao, M., Zhang, X., Chen, S., et al. (2010). Receptor-like cytoplasmic kinases integrate signaling from multiple plant immune receptors and are targeted by a *Pseudomonas syringae* effector. Cell Host Microbe *7*, 290–301.